Nanoscale Advances

REVIEW

View Article Online
View Journal | View Issue

Cite this: *Nanoscale Adv.*, 2021, **3**, 4646

Application of polyoxometalates in photocatalytic degradation of organic pollutants

Jin Lan,† Yu Wang,† Bo Huang, * Zicheng Xiao * and Pingfan Wu *

Received 31st May 2021
Accepted 24th June 2021

DOI: 10.1039/d1na00408e

rsc.li/nanoscale-advances

Organic pollutants are highly toxic, accumulative, and difficult to degrade or eliminate. As a low-cost, high-efficiency and energy-saving environmental purification technology, photocatalytic technology has shown great advantages in solving increasingly serious environmental pollution problems. The development of efficient and durable photocatalysts for the degradation of organic pollutants is the key to the extensive application of photocatalysis technology. Polyoxometalates (POMs) are a kind of discrete metal-oxide clusters with unique photo/electric properties which have shown promising applications in photocatalytic degradation. This review summarizes the recent advances in the design and synthesis of POM-based photocatalysts, as well as their application in the degradation of organic dyes, pesticides and other pollutants. In-depth perspective views are also proposed in this review.

1. Introduction

Human beings enjoy the unprecedented convenience and speed of daily life, benefiting from fast industrial progress, but accompanied by increasingly serious environmental problems.[1–3] In particular, organic pollutants have become one of the major challenging tasks in environmental science due to their high toxicity, strong accumulation, and hard-to-degradability. According to previous ecological investigations, organic pollutants in soil and water have existed for a long time. They are not only difficult to biodegrade, but also have a high migration rate and can spread to all parts of the world including Antarctica and the Arctic.[4,5] It should be noted that organic pollutants can spread to the food chain and accumulate in animals, plants, and humans.[6] They can also cause allergies, birth defects, and cancer, and even damage the immune system and reproductive organs. Even in low concentrations, they will directly affect the body's endocrine system. Hence, it is necessary to find a suitable method to remove such a threat as soon as possible.[7–10] The degradation of organic pollutants with semiconductor photocatalysts especially on n-type semiconductors (such as CdS,[11–13] TiO_2,[14–16] and ZnO[17–19] with an appropriate band gap) has made considerable progress because these photocatalysts can efficiently convert solar energy into chemical energy and promote redox reactions.[20–22] However, electrons and holes easily recombine together, leading to a low photocatalytic performance in the next step.[23–25]

Polyoxometalates (POMs) are metal–oxygen anion nanoclusters which consist of abundant oxygen atoms and early transition metals (including Mo, W, V, Nb, and Ta) in the highest

Institute of POM-based Materials, Hubei Provincial Key Laboratory of Green Materials for Light Industry, Hubei University of Technology, Wuhan, 430068, China. E-mail: huangb2013@126.com; zichxiao@hotmail.com; pingfanwu-111@163.com

† These authors contributed equally to this work.

Jin Lan is an undergraduate student in the Institute of POM-based Materials, Hubei University of Technology (HBUT), and his major is Chemical Engineering and Technology. He has been engaged in the synthesis of POM-based inorganic–organic hybrid materials since he entered HBUT in 2020. Currently, his research work mainly focuses on POM-based molecules and/or nanocomposites and their application in photocatalytic degradation.

Yu Wang received her bachelor's degree in chemical engineering and technology in 2018 from Zhengzhou University of Light Industry. Presently, she is a third year postgraduate student at HBUT and her major is applied chemistry. Her recent research involves organic–inorganic functionalized POM materials, and she mainly focuses on synthesis and performance studies of these compounds including the HER, OER, and biological activities.

oxidation state.[26–30] POMs are usually prepared through the condensation procedure of metal salts in solution (generally in water) at an appropriate pH value and temperature.[31–34] For further feasible applications, the functionalization of pure inorganic POMs is significant because it can regulate the physical and chemical properties of POMs to meet the requirements. Generally, there are three main strategies to functionalize POMs:[35] (1) exchange the counterions of POMs (POMs usually possess negative charges) with organic cations to adjust the solubility of POMs;[36,37] (2) POMs have abundant surface oxygens and can be used as inorganic ligands to coordinate with metal ions and build up high-dimensional coordinated complexes;[38,39] (3) POMs can be covalently modified using organic ligands, which is conducive to the rational design of POM-based inorganic–organic hybrid materials.[40] Apart from the structural diversity and convenient synthesis methods, POMs with excellent physicochemical properties have broad applications in photo-/electro-catalysis, pharmacy, magnetism, and energy storage/conversion.[41–44] In recent studies, POMs are regarded as promising candidates for the efficiently photocatalytic degradation of organic pollutants because of their semiconductor-like properties.[45–48] There are numerous advantages of using POMs as photocatalysts:

(1) POMs are rich in transition metals (such as Mo, W, V, Nb, and Ta), and a large number of potential active sites are exposed on the surface;

(2) The band gap of POMs can be adjusted by changing the heteroatoms (such as P and Si) or adjusting the valence states of metal atoms in their structures to further improve the photocatalytic performance;

(3) POMs can be functionalized using organic ligands and/or loaded on matrix materials (such as TiO_2, carbon nanomaterials, and other support materials), which are conducive to achieving a synergistic effect between different components;

(4) The molecular structure of POMs can be definitely determined by single crystal X-ray diffraction, which is beneficial to the exploration of structure–function relationship at atomic resolution.

Therefore, there is increasing research on POM-based photocatalysts for the photodegradation of organic pollutants, including the structural design, photocatalytic characterization, and the investigation of transformation mechanism and kinetics. In particular, recent reports demonstrate that POM-based photocatalysts can deliver outstanding activity and durability in degrading organic dyes, organic pesticides, and other pollutants. These studies deserve to be systematically summarized and discussed. In this review, we focus on the preparation and structure of POM-based photocatalysts, as well as their application in the degradation of organic pollutants. The influence of POM structures, organic modifications and carriers on the photocatalytic behavior of the catalysts is also discussed. In the end, remarks on the outlook and future challenges of POM-based photocatalysts are also proposed, providing a perspective for researchers who are interested in POM chemistry and environmental protection.

2. Photocatalytic mechanism of POMs

POMs have a semiconductor-like electronic structure, which contains an electron-occupied valence band (VB) and an unoccupied conduction band (CB). In general, as shown in Fig. 1a,

Bo Huang received his bachelor's degree in chemical engineering and technology from the Institute of POM-based Materials, HBUT. Later, he received his master's degree in physical chemistry under the supervision of Prof. Peng Jiang and Minghui Liang from the National Center for Nanoscience and Technology (NCNST), University of Chinese Academy of Sciences (UCAS). His research work mainly focuses on nanomaterials and inorganic–organic hybrid materials, and their applications in energy storage and conversion.

Prof. Zicheng Xiao received his bachelor's and PhD degrees in physical chemistry from Peking University (supervisor: Prof. Yuan Wang). Later, he worked as a post-doctoral fellow in Tsinghua University (supervisor: Prof. Yongge Wei) and worked as a visiting scholar in Lehigh University (supervisor: Prof. Tianbo Liu). Now, he is working in the Institute of POM-based Materials, HBUT, and his current research focuses on POM-based hybrid materials, organic functionalization, single crystal X-ray diffraction, and catalysis.

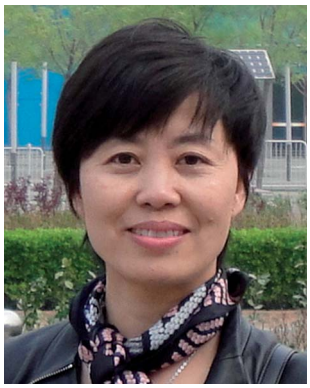

Prof. Pingfan Wu, the founder of the Institute of POM-based Materials in HBUT, obtained her bachelor's and master's degrees from Central China Normal University. She joined HBUT in 2003 and engaged in the field of POMs. She has devoted herself to POM research for more than ten years, and is currently committed to the synthetic development and functional application of POM derivatives.

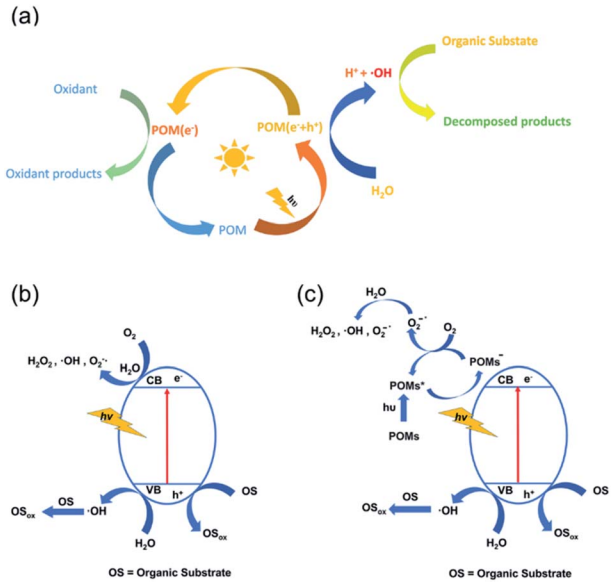

Fig. 1 (a) Diagrammatic scheme of the photocatalytic mechanism of POM-based catalysts; (b) the mechanism of pure POM photocatalysts; (c) the photocatalytic mechanism of POM/support composites.

the photocatalytic mechanism of POM catalysts is similar to that of the TiO_2 catalyst: when the catalyst is irradiated with energy equal to or higher than its band gap, the electrons in its VB are excited to the CB, resulting in photogenerated holes (h^+) and electrons (e^-). The positive holes will produce hydroxyl radicals ($^{\bullet}OH$) with organic substrates in the presence of water. The hydroxyl radicals have strong oxidizing properties and have been proposed as active species for the oxidation and degradation of organic substrates (Fig. 1b).[49] The photocatalytic activity of POMs can be further enhanced when they are loaded on photocatalytically active semiconductors such as TiO_2. In this case, POMs usually act as a scavenger, gathering photogenerated electrons from the semiconductor and becoming a reduced POM^- species. This process delays the recombination of h^+ and e^- pairs and makes the production of hydroxyl radicals by h^+ from the semiconductor more efficient. Meanwhile, the POM^- species transfers an electron to the dissolved oxygen in the solution to generate oxygen radicals $O_2^{-\bullet}$, which then react with water to yield $^{\bullet}OH$ and/or H_2O_2 species, further oxidizing the organic substrates (Fig. 1c).[50] Due to the suitable band gap, good stability, and convenient preparation, Keggin-type POMs are widely applied in the photocatalytic degradation of organic pollutants. Other types of POMs also have potential applications after adjusting the band gap by reasonable modification and loading.

3. Photocatalytic degradation of organic dyes

Organic dyes are the major kind of water pollutants from various sources such as paper making, textile dyeing, cosmetics, paints, food processing, and so on. The total annual output of synthetic dyes exceeds 700 000 tons, of which 15% is discharged into water. Only 47% of the synthetic dyes are biodegradable, and conventional wastewater treatment technologies usually require a long operation time and may produce secondary pollutants. The discharge of dyes has become a serious environmental problem. Photocatalytic degradation is a promising way to overcome this challenge. POM-based catalysts have been applied in the photodegradation of dyes for a long period. Many POMs, especially Keggin-type clusters, have shown high photocatalytic activity for dye degradation, but they are rarely put to practical use. It is still necessary to explore more efficient and stable POM-based photocatalysts. The improvement of the POM photocatalysts has several directions: construct a porous structure to increase the specific pore structure of POMs; modify POMs with suitable organic ligands or substrates to increase the light absorption in the visible region; enhance the separation and reduce the recombination of photoinduced electron–hole pairs through the interactions between POMs and organic ligands or supports. Recent advances in this area are summarized in this section.

3.1 Pure POM photocatalysts

For most of the classic POMs, the light absorption mainly lies in the ultraviolet region. However, ultraviolet light only possesses 5% of the total solar energy reaching the Earth's surface. Thus POM photocatalysts often exhibit relatively low solar energy utilization efficiency. Fortunately, the light absorption properties of POMs can be adjusted by suitable modifications, such as introducing different heteroatoms or attaching to organic ligands. The transition-metal substituted POMs may be more promising candidates than the classic POMs due to their tunable light absorption properties.[51,52] Moreover, the transition metal heteroatoms can provide a catalytic center for photocatalytic reactions. For example, Wang and coworkers studied the photocatalytic properties of Fe(III)-substituted Keggin-type POM $PW_{11}O_{39}Fe(III)(H_2O)^{4-}$(PW11Fe) under visible light irradiation (Fig. 2).[53] This catalyst exhibited high activity in the photodegradation of Rhodamine B (RhB) and nitrobenzene (NB). In a homogeneous reaction, it can completely degrade RhB in 80 min. The mechanism study revealed that the iron heteroatom played a key role in the catalytic process. On visible light excitation, charge transfer occurred from the HOMO of PW11Fe, which is mainly composed of the p orbital of the terminal oxygen, to the iron d orbital at the site of H_2O complexing with Fe(III), resulting in the oxidation of H_2O molecules and the production of hydroxyl radicals. Hydroxyl radicals are strong oxidants that further lead to the decomposition and mineralization of organic dyes. On the other hand, the Fe(III) center was reduced to unstable Fe(II), which then reduced the dissolved oxygen molecules to H_2O_2 and restored to Fe(III) itself. In addition, this photocatalyst also showed good stability and can be reused five times without significant loss of activity. This work demonstrates that transition metal substituted POMs are more promising visible-light-driven photocatalysts for dye degradation.

The applications of large POM clusters have attracted increasing attention in recent years. These high-nuclear metal-

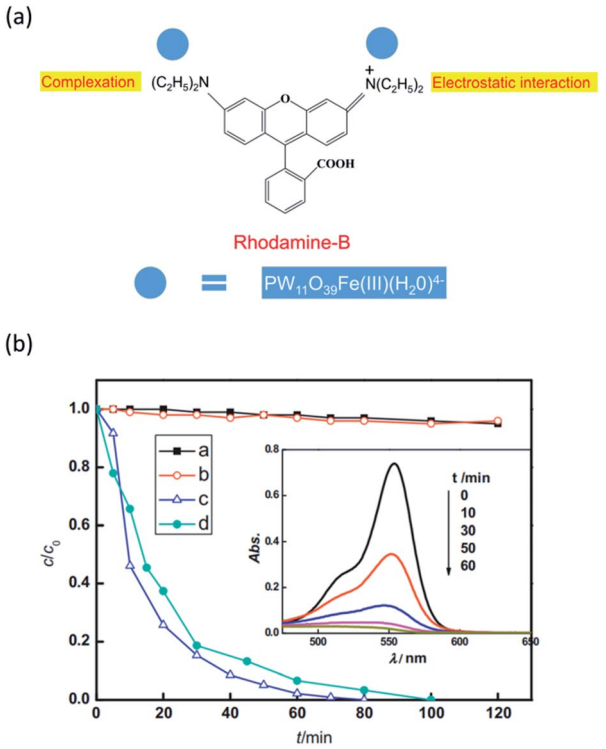

Fig. 2 (a) Illustration of the interaction between PW11Fe and RhB; (b) photocatalytic degradation of RhB and NB under visible-light irradiation, black line: RhB under visible-light irradiation; red line: RhB and PW11Fe under dark conditions; blue line and inset graph: RhB and PW11Fe under visible-light irradiation; green line: NB and PW11Fe under visible-light irradiation. Reproduced with permission from ref. 53. Copyright© 2012 Elsevier.

oxo clusters usually have wheel-like or hollow spherical structures which can provide large anionic cavities as effective "reactors" for the catalytic reaction[54] In 2020, Zhang and coworkers prepared a series of transition metal substituted wheel-like clusters $K_xNa_yH_{26-x-y}[\{TM(H_2O)_3(SnR(H_2O))_2(\mu\text{-}OH)(\mu\text{-}SnR(H_2O))\}_2(P_8W_{48}O_{184})]\cdot nH_2O$ (TM_2-Sn_6-P_8W_{48}, R = CH_2CH_2COO; TM = Mn, Co, Ni; x = 0, 1, 2; y = 19, 22, 15; n = 72, 85, 75, respectively) through a three-step procedure.[55] These clusters exhibited visible light absorption originating from the transition metal ions. They also showed high photocatalytic activities for RhB degradation with a maximum efficiency of nearly 100% in 3 h. Moreover, the reaction rate constants of TM_2-Sn_6-P_8W_{48} were 2.3 times greater than those of the P_8W_{48} cluster without transition metal heteroatoms, indicating that transition metals played an important role in the photocatalytic process. When these photocatalysts were loaded on TiO_2, they not only maintained high activity, but also showed good reusability. However, the degradation efficiency of RhB decreased slightly after each cycle, probably due to the partial leaching of the catalyst and the absorption of dyes onto the catalyst's surface. This work opens a new direction for exploring new efficient POM-based photocatalysts.

POMs are usually crystalline materials, thus POM catalysts often suffer from the disadvantage of low specific surface area. One solution to this problem is to prepare nanosize crystals.[56] Although various synthetic protocols for such nanocrystals have been developed in the past decade, there is still a lack of general methods for controlling the morphology of the POM nanostructures. Recently, Pang's group reported the preparation of $K_3PW_{12}O_{40}\cdot nH_2O$ nanocrystals under hydrothermal conditions using KCl and phosphotungstic acid as raw materials.[57] Interestingly, the SEM images revealed that the reaction temperature and time played important roles in the growth of these nanostructures. When the reaction was carried out at 140 °C for 12 h, uniform hollow rhombic dodecahedral nanocrystals were obtained. When decreasing the reaction temperature to 120 °C and 100 °C, the reaction resulted in rhombic dodecahedral and semi-hollow spherical nanostructures, respectively. The photocatalytic activities of these nanocrystals were evaluated by RhB degradation experiments with activated H_2O_2. The results showed that the hollow rhombic dodecahedral nanocrystals performed best in terms of degradation speed, efficiency, and recycling ability. RhB completely degraded after 90 min under visible light irradiation. These porous nanocrystals are promising photocatalysts for practical wastewater treatment.

3.2 POM-based organic–inorganic hybrid photocatalysts

Organic modification of POMs is one of the most important research topics in POM chemistry because it can tune the physicochemical properties of POMs. POM-based inorganic–organic hybrids have potential applications in various fields. In the field of photocatalysis, POM hybrids also show significant advantages: the organic ligands can extend the light absorption performance of POM clusters to the visible region, thereby improving the utilization of sunlight; metal–organic species can tune the band gap between the HOMO and LUMO of POM clusters to improve the photocatalytic properties of the hybrid material; porous structures can also be constructed from the organic moiety to increase the surface area of the hybrid catalyst.[58] However, stability is a main drawback of POM-based organic–inorganic hybrids. Only a few hybrid catalysts are stable for a long time under photocatalytic conditions to date.[59]

In 2018, Peng and coworkers reported three POM-based organic–inorganic hybrid compounds $[Cu(PBI)_2(H_2O)][\{Cu(PBI)(OH)(H_2O)\}\{PW_{12}O_{40}\}]\cdot 5H_2O$, $[Cu(PBI)_2(H_2O)][\{Cu(PBI)_2(H_2O)\}\{SiW_{12}O_{40}\}]\cdot 4H_2O$ and $[Cu_4(HPO_4)(PO_4)(H_2O)_2(PBI)_4][PMo_{12}O_{40}]\cdot H_2O$ (PBI = 2-(pyridin-2-yl)-1*H*-benzo[*d*]imidazole).[60] In the crystal structure of these hybrids, the {Cu/PBI} cations are stacked into 3D supramolecular frameworks *via* π–π and OH–π interactions. It is interesting that these hybrids all exhibited selective photocatalytic activity for the degradation of organic dyes. These photocatalysts showed high degradation rates (all above 95%) for the degradation of methylene blue (MB). However, they were less active in the photodegradation of RhB with degradation rates all below 80%. The difference in photocatalytic activities may come from the different adsorption capacities of organic dyes. Because RhB has a larger molecular size, it did not match the pore of the catalyst and was difficult to adsorb on the catalyst. Especially, $[Cu_4(HPO_4)(PO_4)(H_2O)_2(PBI)_4][PMo_{12}O_{40}]$ had the lowest structural porosity and it only showed a 43.87% degradation rate for

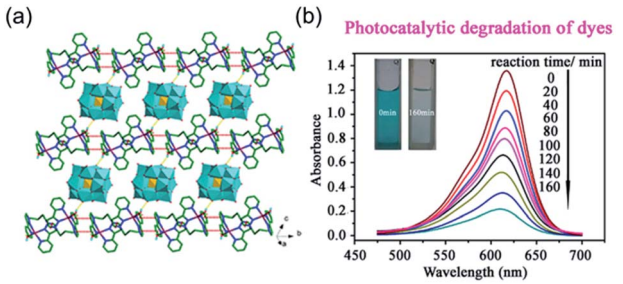

Fig. 3 (a) Crystal structure of $[Ag_4(H_2O)(L)_3(SiW_{12}O_{40})]$ (L = 1,4-bis(3-(2-pyridyl)pyrazol)butane); (b) UV-vis absorption and photocatalytic degradation of MG. Reproduced with permission from ref. 61. Copyright© 2016 Elsevier.

RhB. This work shows the possibility of selective degradation of small organic dyes by the precise design of a POM-based hybrid photocatalyst with pores of suitable size.

As shown in Fig. 3, Ma's group reported a polyoxometalate-based inorganic–organic hybrid $[Ag_4(H_2O)(L)_3(SiW_{12}O_{40})]$ (L = 1,4-bis(3-(2-pyridyl)pyrazol)butane).[61] Surprisingly, this crystalline photocatalyst showed high activity for the heterogeneous degradation of MB and malachite green (MG) with degradation rates of 83% and 81% within 160 min, respectively. The high photocatalytic activity may be contributed by the large $[Ag_4(H_2O)(L)_3]^{4+}$ cation, which supports the transportation of excited holes/electrons to the surface. Besides, three conformations of L ligands with different lengths linked by Ag(I) atoms with lower enthalpy prohibit the conglomeration and deactivation of POMs and further enhance their photocatalytic properties. This catalyst can be recycled easily and no significant loss of activity was observed after 5 cycles. In addition, this catalyst can also reduce Cr(VI) in wastewater using isopropanol as a scavenger. It is worth mentioning that this catalyst is used in the crystalline state. There is still great potential to enhance its photocatalytic efficiency by lowering its crystal size or loading it on a suitable support.

Organic modification gives POMs enormous potential in future applications. However, due to the vulnerability of organic moieties under photocatalytic conditions, it is difficult to acquire durable hybrid photocatalysts. The design and synthesis of efficient and stable POM hybrid photocatalysts is still a challenging task. More efforts are needed to develop advanced synthetic methods and illustrate the relationship between photocatalytic activity and organic moieties.

3.3 POM-based composites

Because POMs are usually highly soluble in water, most of the photocatalytic reactions of POMs are homogeneous, and the separation and recycling of the catalyst are difficult. In heterogeneous catalysis, POMs also encounter problems such as low surface area and easy leaching. Supporting POMs on suitable carriers is the main strategy to overcome these shortcomings. Moreover, the synergistic effect between POMs and the carriers may even enhance the photocatalytic properties. In the past few decades, researchers have successfully supported POMs on different carriers such as TiO_2, organic polymers, MOFs, carbonitride, *etc.* These POM-based composites have shown enhanced photocatalytic performances and are expected to be used in the degradation of organic dyes.

3.3.1 POMs/TiO_2 composites. TiO_2 is the most widely studied photocatalytic material by far, because of its high stability, easy availability, nontoxicity, and low cost.[62,63] However, the practical application of TiO_2 is severely limited by its fast electron–hole recombination and low absorption of visible light due to its wide band gap.[64] The combination of TiO_2 and POMs is considered to be one of the solutions to these problems.[65] POMs can be used as mediators which can control the dynamics of photo-induced electron transfer from the conduction bands of TiO_2. They can also be good electron acceptors which can receive the photo-generated electrons from TiO_2 and avoid electron–hole recombination. On the other hand, the loading of POMs on TiO_2 nanoparticles also increases the surface area of POMs and enhances their photocatalytic properties.[66] Many reports have demonstrated that the loading of POMs can significantly improve the photocatalytic activity for dye degradation.[67–73] However, a lot of work also demonstrated that a high loading content of POMs on TiO_2 will decrease the activity. There may be several reasons for this phenomenon: the excess POMs block the pore of the catalytic material; the POMs compete for active sites on the catalyst surface; the inner-filter effect of POMs will reduce light absorption. Therefore, the support ratio of POMs must be strictly controlled when designing POM/TiO_2 composites.

At present, the improvement of POM/TiO_2 composites mainly focuses on the design of TiO_2 carriers. For example, TiO_2 nanoparticles with large holes and surface area could support more POMs without loss of activity. For example, Guo's group successfully loaded Keggin-type POMs $[(C_4H_9)_4N]_5PW_{11}CoO_{39}$ on ordered mesoporous TiO_2 nanoparticles by an evaporation-induced self-assembly method (Fig. 4).[74] $EO_{20}PO_{70}EO_{20}$(P123) was used as a template to prepare well ordered mesoporous TiO_2, which can maintain a large surface area after the loading of POMs. UV-vis spectra of the composites showed that the light absorption of TiO_2 has a significant red-shift to the visible region after the loading of POMs. The composites displayed

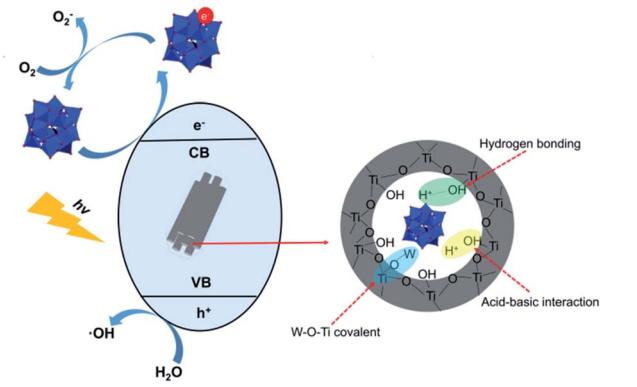

Fig. 4 Structure and photocatalytic mechanism of the $H_3PW_{12}O_{40}$/TiO_2 composite material.[74]

higher photocatalytic degradation activity for methyl orange (MO) under solar simulating Xe lamp irradiation compared with pure TiO_2. When the percentage of POM loading reached 32.3%, the composite exhibited the highest photocatalytic activity and MO was completely degraded after 90 min.

Recently, multi-component photocatalysts have brought new horizons to the classic POM/TiO_2 composites. The introduction of other components, such as transition metal ions or organic polymers, may further enhance the activity of the photocatalyst. In 2017, Khoshnavazi successfully loaded a sandwich-type POM $K_{10}H_2[(OCe^{IV})_3(PW_9O_{34})_2]\cdot xH_2O$ (PWCe) onto a series of lanthanide-doped TiO_2 (Ln–TiO_2; Ln = Pr, Nd, Sm, Eu, Tb) nanoparticles by a simple impregnation method.[75] The introduction of Ln ions has two significant effects: the Ln ions can enhance the electron trapping effect and further delay the electron–hole recombination; they also provide empty f-orbitals for the coordination of organic pollutants and improve the adsorption on TiO_2 surface. Meanwhile, the loaded PWCe can capture the photogenerated electrons and further impede the charge–hole recombination. The photodegradation experiment of MO showed that 10% loading of PWCe significantly improved the photocatalytic properties of the catalysts, resulting in degradation rates all higher than 90%, while the degradation rate of Ln–TiO_2 composites without PWCe was only 40–60%. The Ln–TiO_2/PWCe catalyst also has good reusability, without obviously losing its activity after five cycles.

Recently, P. Wu *et al.* designed and prepared a novel multi-component photocatalyst Fe_3O_4@TiO_2@PDA/SiW_{11}V–Ag, which degraded MO completely under simulated solar light irradiation in 120 min.[76] In this catalyst, TiO_2 is an active species to protect the Fe_3O_4 from corrosion and oxidation; the $[SiW_{11}VO_{40}]^{6-}$ is another active component and electron reservoir that can enhance the electron–hole separation of TiO_2; the PDA acts as a conductive linker, which improves the electron transfer between components, and it also enhances the light absorption capacity of the composite in ultraviolet and visible region; Ag nanoparticles play a key role in enhancing the activity by providing electron trapping ability. The trapped electrons in Ag nanoparticles can further reduce O_2 to generate O_2^- active species which can directly oxidize MO to degraded products. Without Ag nanoparticles, the catalyst only showed a 29% degradation rate under similar conditions. Finally, magnetic Fe_3O_4 particles contribute to the convenient separation and recycling of the catalyst. This catalyst demonstrated the great potential of multi-component POM@TiO_2 composites in photodegradation, and provides a new way for achieving highly efficient and durable photocatalysts for practical wastewater treatment.

POMs can also act as a switchable reductant for the decoration of metal nanoparticles onto the surface of TiO_2 nanotubes. Bansal and coworkers reported a series of decorated TiO_2 nanotubes with metal nanoparticles and POMs.[77] These composites were prepared by a three-step protocol: firstly, Keggin-type phosphotungstic acid $[PW_{12}O_{40}]^{3-}$ (PTA) was loaded on TiO_2 nanotubes to form TiO_2–PTA composite materials; then, in the presence of isopropanol, under UV light irradiation and nitrogen protection, the PTAs were reduced to

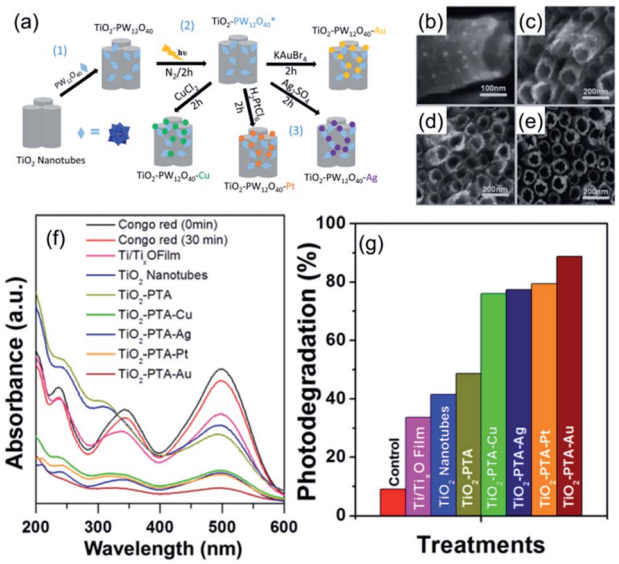

Fig. 5 (a) Preparation of TiO_2–PTA composite materials; (b–e) morphological characterization of TiO_2–PTA composite materials by SEM; (f) UV-vis spectra of Congo red by photocatalytic degradation for 30 min; (g) photodegradation of Congo red expressed as reduction at 500 nm with different POM-based photocatalysts. Reproduced with permission from ref. 77. Copyright© 2018 American Chemical Society.

$[PW_{12}O_{40}]^{4-}$(PTA*); finally, the metal salts of $CuCl_2$, Ag_2SO_4, H_2PtCl_6, or $KAuBr_4$ were introduced into the composite and subsequently reduced *in situ* by the surface bounded PTA* (Fig. 5). These metal nanoparticle decorated TiO_2 nanotube/PTA composites exhibited excellent photoreduction properties for Congo red under simulated solar light. TiO_2–PTA–Au nanotubes were the most active composite, which resulted in *ca.* 89% degradation. The metal nanoparticles can suppress the influence of the charge-recombination phenomenon and increase the lifetime of the electron–hole pair, thereby enhancing the photocatalytic activity of the composite.

3.3.2 POM-based metal–organic frameworks (POMOFs). The incorporation of POMs into MOFs has become an important direction for designing POM-based catalysts.[78–81] Fixing POMs on porous MOF structures can increase the surface area while maintaining their excellent catalytic performance. There are two strategies for incorporating POMs into the MOF structure: (1) introducing POMs as a sub-unit to construct the MOF structure; (2) encapsulating POMs into the framework to form a host–guest structure. The second strategy is more accessible because POMs have a fertile oxygen surface and can coordinate with metal ions or form hydrogen bonds with organic ligands. Such POM/MOF composites have also been applied in photocatalysis dye degradation.[82–92] Besides the advantages of large surface area and high catalytic activity, MOFs with suitable organic ligands can absorb visible light and improve the light utilization rate of POM-based photocatalysts.

In a recent report, Fu's group encapsulated Keggin-type POM $[PW_{12}O_{40}]^{3-}$ in a copper–viologen framework (Fig. 6). This new composite showed a wide light absorption range from the ultraviolet to near-infrared region.[93] Photoelectrochemical analysis showed that the composite had a high efficiency of

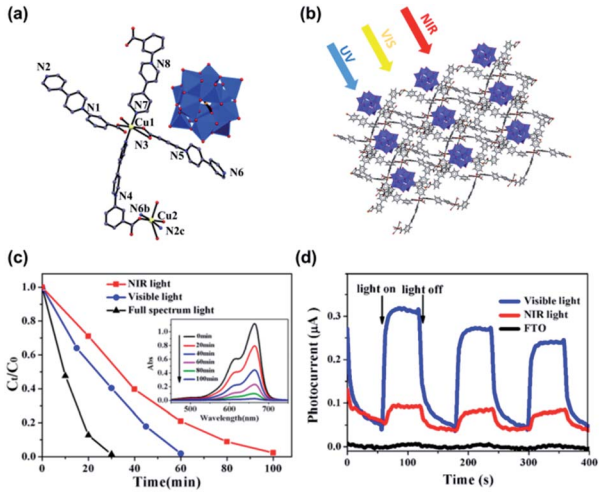

Fig. 6 (a and b) The single molecule diagram and packing model of Keggin-type POMs $[PW_{12}O_{40}]^{3-}$ in a copper–viologen framework. (c) Degradation rates of MB under different conditions (inset: UV-vis spectra under NIR light); (d) photocurrent responses under visible light, NIR light, and the FTO glass under NIR light (benchmark). Reproduced with permission from ref. 93. Copyright©2018 American Chemical Society.

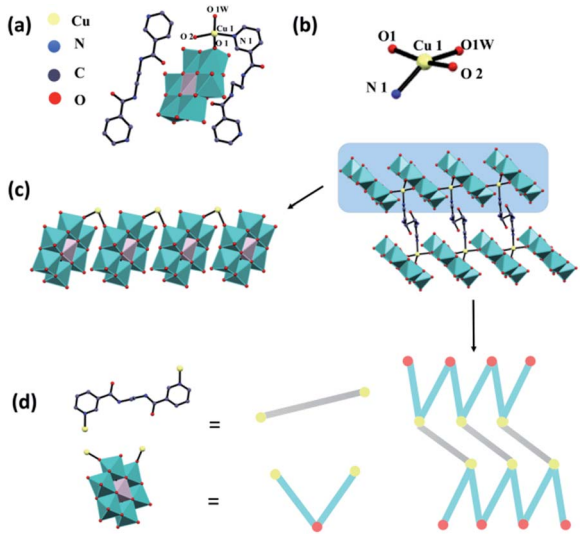

Fig. 7 (a) The single molecule, (b) partial enlarged drawing of the Cu coordination site, (c) packing model, and (d) the ball-stick model of the Anderson-type polyoxomolybdate $H\{CuL_{0.5}^{1}[CrMo_6(OH)_6O_{18}](H_2O)\}\cdot 0.5\ L^1$ (L^1 = *N*,*N*′-bis(3-pyridinecarboxamide)-1,2-ethane).[95]

electron–hole pair generation, which is the first and most essential step of a photocatalytic reaction. The composite also showed high photocatalytic activity for the degradation of methylene blue (MB). In the presence of this photocatalyst, under the irradiation of visible and NIR light, respectively, about 98.2% of MB was degraded within 60 min, and around 97.7% of MB was degraded in 100 min.

POMs have a large size and are usually difficult to package in framework structures. Thus the choice of organic ligands is critical to the design of POMOFs. Pyrazine ligands have flexible coordination modes and small steric hindrance, and are suitable for the construction of POMOFs. The POMOFs based on metal–pyrazine frameworks have shown potential applications in photocatalytic degradation. Recently, Zhou and coworkers reported three novel Keggin-type POM anchored Ag–pz frameworks (pz = pyrazine).[94] The resulting composites had high specific surface area, and showed high photocatalytic activities in degrading RhB and MB with a degradation rate of 95% approximately. In addition, these composites also had high specific capacitances that they can be used as electrode materials in supercapacitors.

Wang and coworkers reported two novel metal–organic complexes based on Anderson-type polyoxomolybdate (Fig. 7).[95] They chose bis-pyridyl-bis-amide ligands to construct such complexes because: (1) the pyridyl and amide groups can provide more potential coordination sites; (2) the amide groups have both N–H hydrogen donor and C=O hydrogen acceptor, thereby promoting the formation of hydrogen bonds; (3) the flexible $-(CH_2)_n-$ spacers can freely bend or rotate when forming coordination bonds or hydrogen bond interactions. These complexes showed high photocatalytic activities for the degradation of RhB and MB, and can be applied as prospective photocatalyst materials for dye degradation.

3.3.3 POMs on other carriers. In 2018, Koohi and coworkers employed natural porous minerals (such as natural zeolite and natural clays) as the carrier of silicotungstic acid (HSiW).[96] The POM was loaded on clinoptilolite (Clin), mordenite (Mord), bentonite (Bent), and kaolinite (Kaoln) by impregnation. Photocatalytic tests revealed that HSiW/Clin had the highest activity for the degradation of MB with a degradation rate of 92% among the four photocatalysts. This is because HSiW/Clin has the highest crystallinity and the smallest crystallite size, both of which greatly affect the photocatalytic properties. The FT-IR results showed that the absorption peaks of silicotungstic acid had a significant shift to lower wavenumbers in the case of clinoptilolite and mordenite supports, indicating that these two photocatalysts have strong interactions with POMs and the support. Mechanism studies revealed that clinoptilolite can transfer electrons to POMs and convert the silicotungstic acid to a strong oxidant $H_5SiW_{12}O_{40}$. On the other hand, covalent bonds were formed between the W atom in HSiW and the Si or Al atom in clinoptilolite (W–O–Al or W–O–Si), which can trap electrons in the conduction band and reduce the electron–hole recombination. These results indicated that clinoptilolite could be an inexpensive, easily accessible support for POMs for photocatalytic degradation of dyes.

Graphitic carbonitride (g-C_3N_4) is a metal-free catalyst with excellent electronic conductivity and great mechanical strength.[97–99] Recently, POM catalysts supported on g-C_3N_4 have attracted increasing attention.[100–102] As shown in Fig. 8, Wang's group reported two novel g-C_3N_4 supported Keggin-type phosphomolybdate (PMo_{12}) and phosphotungstate (PW_{12}) photocatalysts, which were prepared by a hydrothermal method.[103] The N_2 absorption tests showed that the specific surface area of g-C_3N_4 increased after incorporating with POMs. The composite POMs@g-C_3N_4 showed a better absorption of MB than pure g-C_3N_4. In photocatalytic degradation of MB, the POMs@g-C_3N_4

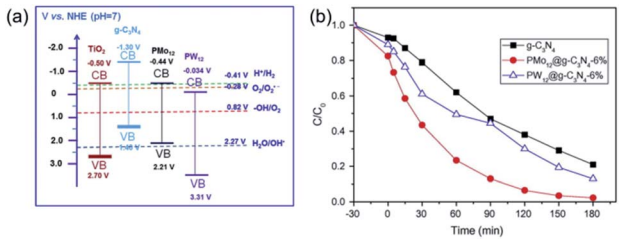

Fig. 8 (a) Band gap and redox potentials of TiO_2, g-C_3N_4, PMo_{12}, and PW_{12} photocatalysts; (b) photocatalytic degradation of MB under UV-vis light irradiation. Reproduced with permission from ref. 103. Copyright© 2015 Elsevier.

photocatalyst demonstrated excellent activity with a degradation rate of nearly 100% in 180 min. Compared to TiO_2, g-C_3N_4 showed more significant differences in band positions. The conduction band of g-C_3N_4 is more negative than that of PMo_{12} and PW_{12}, while the valence band is less positive than that of POMs, resulting in higher charge transfer efficiency and photoinduced charge separation rate. Therefore, the photocatalytic activity of POMs@g-C_3N_4 was remarkably enhanced. This work proves that g-C_3N_4 is a promising carrier for POM-based photocatalysts.

Graphene is a two-dimensional nano-carbon material that is considered to be an ideal support for catalysts due to its extremely large specific surface area, excellent electron transfer properties, high mechanical strength, and chemical stability.[104] Graphene oxide(GO) is considered to be an excellent support for POM photocatalysts because it can not only increase the specific surface area of POMs, but also avoid the electron–hole recombination and enhance the photocatalytic properties.[105,106] However, the combination of POMs and GO is mainly *via* non-covalent bonds, such as physical adsorption, hydrogen bonding, and electrostatic interaction. Thus these catalysts often face the problem that the POMs are easily detached from the substrate. Recently, Wang and coworkers reported a novel POM@GO photocatalyst by grafting a single lacunary Dawson-type phosphotungstate $K_{10}[\alpha\text{-}P_2W_{17}O_{61}]\cdot 20H_2O$ onto GO *via* covalent bonding.[107] GO was first modified with 3-aminopropyltrimethoxysilane to obtain amino-containing graphene oxide (GO–NH_2). Then P_2W_{17} reacted with γ-glycidoxypropyltrimethoxysilane to produce P_2W_{17}-EPO with epoxy groups. Finally, the ring-opening reaction between GO–NH_2 and P_2W_{17}-EPO resulted in the GO/P_2W_{17} composite. BET analysis demonstrated that GO/P_2W_{17} had a larger specific surface area 5 times than that of P_2W_{17}-EPO. Electrochemical impedance spectroscopy (EIS) showed that the charge transfer resistance of GO/P_2W_{17} was much lower than that of P_2W_{17}. This result indicated that GO carriers can effectively improve the separation of photoinduced electron–hole pairs and the rapid transfer of photoinduced electrons at the GO/P_2W_{17} interface, leading to the increase of photocatalytic activity. The photocatalytic MB degradation experiment demonstrated the high photocatalytic activity of GO/P_2W_{17}: under optimal conditions, 94.3% of MB was degraded in 90 min. This photocatalyst also showed good stability and no obvious decrease in the degradation rate was observed after 5 cycles.

4. Photocatalytic degradation of organic pesticides

In modern agriculture, pesticides are extensively used to control weeds, animal pests, or plant diseases. Pesticides and their intermediate products during the degradation process are usually toxic; some of them are harmful to the human body even in trace amounts. Due to their aqueous solubility and long-term degradation, the remaining pesticides in the soil can enter the surface and underground water, further be concentrated in vegetables and animals, and finally move up to the food chain, causing serious threats to environmental safety and public health. Compared to organic dyes, organic pesticides are usually more stable and difficult to detect and remove from the water system by traditional treatment.[108] Photocatalytic degradation is regarded as a promising method for the removal of organic pesticides in water. Some semi-conductive photocatalysts, such as TiO_2 and ZnS, have been widely studied and reviewed in previous literature.[109,110] There are also some research studies utilizing POMs as photocatalysts for the degradation of pesticides such as lindane and imidacloprid.[111–113] Recently, POM photocatalysts also exhibited good activities for the degradation of persistent pesticides such as aromatic pesticides.

2-(1-Naphthyl)acetamide (NAD) is a widely-used plant growth regulator which shows prolonged natural degradation and is harmful to aquatic organisms. In 2017, Wong-Wah-Chung and coworkers applied the decatungstate anion $[W_{10}O_{32}]^{4-}$ to the degradation of NAD.[114] The results showed that $[W_{10}O_{32}]^{4-}$ had an excellent activity for photocatalytic degradation of NAD. After UV light (365 nm) irradiation for 22 h, 95% of NAD was degraded in the presence of $[W_{10}O_{32}]^{4-}$, while only 5% loss of NAD was observed in the absence of POMs. When the experiment was carried out under simulated solar light irradiation, a degradation rate of 89% was recorded in the presence of $[W_{10}O_{32}]^{4-}$. Moreover, NAD was converted to CO_2, H_2O, and nitrates at the end of the photocatalytic degradation. Mechanism studies indicated that the photo-excited decatungstate decays to a longer-lived, extremely reactive, and non-emissive transient, which then takes an electron from NAD, leading to the formation of $NAD^{\cdot+}$ radicals (Fig. 9). These radicals subsequently react with water, forming a series of hydroxylated products, which further lead to the opening of the aromatic ring. The resulting aliphatic derivatives can further be oxidized to CO_2 and H_2O. The work proves that POMs can be applied as efficient photocatalysts for the degradation of aromatic pesticides.

In 2019, Xia's group reported a novel photocatalyst based on phosphotungstate supported on polyimides.[115] The catalyst was synthesized by an *in situ* solid-state polymerization of pyromellitic dianhydride and the melamine modified phosphotungstate, which was first prepared by mixing an aqueous solution of melamine and phosphotungstic acid and heating at 90 °C. The XRD patterns revealed that this catalyst had an alternate stacking structure of polyimides and phosphotungstates. The XPS results indicated that there were strong interactions between polyimide and phosphotungstate, which immobilized the POMs and established a stable electron transfer channel from polyimide to

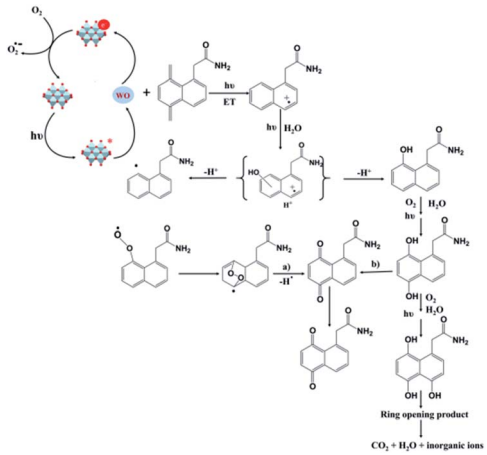

Fig. 9 Photocatalytic mechanism of $[W_{10}O_{32}]^{4-}$ in the degradation of NAD.[114]

phosphotungstate in the composites. UV-vis spectroscopy showed that the light absorption of the composite extended from 350 nm to over 800 nm, indicating intense electron delocalization between the POM unit and the conjugated polyimide. This photocatalyst exhibited excellent photocatalytic activity for the degradation of imidacloprid. Under visible light irradiation, 72.4% of imidacloprid was degraded in the presence of the composite after 3 h, while no obvious degradation was observed using melamine modified POMs or polyimides individually. Mechanism studies revealed that the significant enhancement of the photocatalytic activity originated from the intense electron delocalization *via* intermolecular POM anions–π interactions, which benefits the photogenerated electron transfer from the conduction band of polyimide to the unoccupied W 5d orbitals of the phosphotungstate, suppressing the electron–hole recombination. The photogenerated holes can efficiently produce hydroxyl radicals, which are the main active species in the photocatalytic oxidation of imidacloprid. In subsequent studies, they prepared a series of carbonitride-supported tungstophosphate composites by thermal treatment of melamine modified phosphotungstates.[116] These catalysts also showed even better performances in the visible-light-driven photocatalytic degradation of imidacloprid with a maximum degradation rate of approximately 85% in 3 h. These research studies contribute a new strategy for the design of POM-based composite photocatalysts for pesticide degradation.

Although POM photocatalysts have a bright future in the degradation of pesticides, the progress in this field is still slow, and the potential of POMs has not been fully exploited yet. More efforts are still needed to illustrate the degradation mechanism of different pesticides and to develop feasible techniques for practical water treatment.

5. Photocatalytic degradation of other organic pollutants

Phenolic compounds are the most common organic pollutants in wastewater released from the petroleum and pharmaceutical industries. Many of them are not biodegradable and can remain toxic for a long period. Photocatalysis degradation has been demonstrated as one of the successful methods for the removal of phenolic compounds in wastewater.[117,118] POMs have already been used as photocatalysts for phenol oxidation for a long time.[119] Recently, significant progress has been made in the degradation of phenolic compounds with POM-based composite photocatalysts.[120–122] Rtimi's group reported a TiO_2/FeO_x/POM nanocomposite as a photocatalyst for the degradation of 2,4-dichlorophenol under visible light.[123] This catalyst exhibited a high degradation efficiency of 76.0% in 3 h. The polyoxotungstate in the composite acts as an electron acceptor which scavenges the photoexcited electrons from TiO_2 and decreases the electron–hole recombination. The introduction of FeO_x can enhance the light absorption in the UV-vis region and accelerate photocatalytic degradation. Their magnetic properties also make the separation and reuse of the catalyst much more convenient. This work shows a subtle design of composite photocatalysts towards practical application.

Antibiotics are widely used in the medical industry today. Every year, large amounts of abandoned antibiotics are discharged into soil and water, causing adverse effects on the environment and ecosystem. The traditional wastewater treatment cannot properly treat the antibiotics and their residues, and thus the photocatalytic technique has been employed to solve this problem.[124] Recently, a few inspirational studies using POMs as photocatalysts for the degradation of antibiotics have been reported. For example, Wang's group reported a series of POM-based composite catalysts with the nitrogen-deficient g-C_3N_x support for the degradation of ciprofloxacin (Fig. 10).[125] These catalysts all exhibited high photocatalytic degradation efficiencies and very fast reaction rates. Especially, the g-C_3N_x/PTA-30 catalyst can remove 97.3% of ciprofloxacin in 5 minutes under visible light irradiation. Doping Keggin-type POMs in porous g-C_3N_4 nanosheets increased the light absorption and the separation efficiency of electron–hole pairs, leading to higher photocatalytic activities. L. Hou and coworkers designed

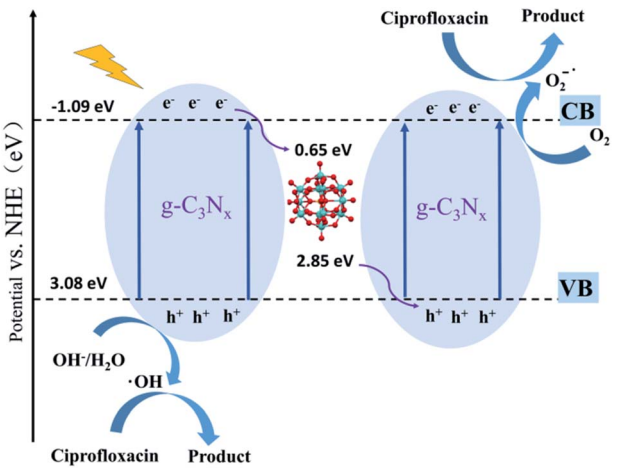

Fig. 10 The photocatalytic mechanism of POM@g-C_3N_4 nanocomposite.[125]

and synthesized an In(III)-based MOF MFM-300 incorporating Keggin-type phosphotungstic acid *via* a novel *in situ* hot-pressing synthesis method.[67] This catalyst showed excellent photocatalytic activity for the removal of PhAC sulfamethazine with 98% degradation efficiency after 2 h in the presence of H_2O_2 under optimal conditions. The catalytic activity of the composite was much higher than that of the individual POM catalyst because of the larger specific surface area, the improved accessibility of H_2O_2 to the active sites, and the promotion of the host–guest electron transfer by the composite structure. These pioneering research studies demonstrated that POM-based composites are promising photocatalytic materials for the degradation of antibiotics in wastewater.

6. Conclusion and outlook

POMs have been demonstrated as a kind of green and economical photocatalyst for the removal of organic pollutants in wastewater. Benefitting from their stable molecular structures and reversible redox properties, POMs possess high catalytic activity and durability in photodegradation. They can also act as efficient electron scavengers in composite photocatalysts. Nevertheless, POMs also have many drawbacks, such as poor visible-light utilization, low specific surface area, easy leaching, and sensitivity to pH. Thus, it still requires great efforts to solve these problems in order to make POM photocatalysts suitable for a wide range of practical applications. This review has summarized the recent advances and listed the challenges in this field. In future exploration, the following points may be taken into consideration:

(1) Although a number of POM photocatalysts have been reported to date, most of them are based on a few classic POM clusters such as Keggin, Dawson, and Anderson. Thus, the potential of POMs has not been fully explored yet.[126] The search for excellent photocatalysts from the tremendous amount of POMs will be an arduous task. On the other hand, there is a lack of mechanism study of POM photocatalytic degradation at the atomic level, which has impeded the design and improvement of POM photocatalysts. Further research studies should focus on the effects of the metal atoms, cage structure, and organic ligands in POM molecules on the key factors related to photocatalytic activity such as light absorption, electron–hole separation, and charge transfer. Such efforts can provide valuable guidelines for the design of highly efficient POM photocatalysts.

(2) The leaching of POMs is one of the main drawbacks that hinder the practical application of POM-based photocatalysts. In the past twenty years, abundant studies have successfully immobilized POMs on various kinds of organic/inorganic supports. However, most of the composites are fabricated through hydrothermal, impregnation, self-assembly, and sol–gel methods, in which the POM clusters are usually attached to the supports *via* non-covalent interactions, and can be removed easily after a few photocatalytic cycles in an aqueous solution. Thus, grafting POMs onto supports *via* covalent bonds could be a better solution for the leaching problem. The fabrication of these composites is far more difficult of course, especially those with inorganic supports. Therefore, new synthetic strategies and protocols are still needed.

(3) Besides the direct application as photocatalysts, POMs are also ideal precursors for the preparation of highly dispersed metal oxide or metal carbide nanoparticles due to their discrete and uniform structure. Compared with the traditional metal composites, the nanoparticles prepared through POM precursors have several advantages: (i) the structure of POM precursors is defined and can be designed at the atomic scale; (ii) the derivatives are nanostructured and can be rationally controlled; (iii) the inherent heteroatoms can be directly doped into the lattices of metal nanocomposites for band gap regulation; (iv) the agglomeration problem of traditional metal composites can be alleviated because there are steric hindrances and electronic repulsion between the POM precursors, ensuring high dispensability during the synthetic procedure.[127,128] Recently, some researchers have utilized these nanoparticles as photocatalysts for efficient photocatalytic degradation of organic pollutants in wastewater.[129] This is a new promising direction that employs POMs as precursor materials to achieve highly efficient nanophotocatalysts.

(4) The investigation of POM-based photocatalysts is rare in the degradation of organic pollutants in the air system such as volatile aldehyde and benzene compounds. To expand the applications of POM-based photocatalysts, a higher BET specific surface area and stronger adsorption/desorption ability are needed. Previous reports reveal that incorporating POMs into polymers (such as MOFs, COFs, and other conductive polymers),[106,130,131] and malleable supports may enhance the interaction between the active sites of POMs and the molecules of organic pollutants. In addition, finding more suitable usage methods is also beneficial to catalytic efficiency. For example, employing POM-based photocatalysts in aerosol or sprayed form may lead to a high conversion rate of pollutants in the air, which is also helpful for practical application and commercialization in the future.

Nevertheless, POMs are promising candidates for the photocatalytic degradation of organic pollutants although there are still some challenges needed to be solved in depth. Recent research studies still propose a bright future for designing advanced POM-based photocatalysts from preparation to applications. With ongoing efforts, more ingenious breakthroughs of POM-based materials are expected in the future, especially in green energy conversion and environmental science.

Conflicts of interest

There are no conflicts to declare.

Acknowledgements

This work was supported by the National Natural Science Foundation of China (No. 21271068 and 21401050). Students' Innovation Project of HBUT (No. S202010500097 and X202110500112)

Notes and references

1 P. Bhatt, S. Gangola, G. Bhandari, W. P. Zhang, D. Maithani, S. Mishra and S. H. Chen, *Chemosphere*, 2021, **268**, 128827.

2 D. Gang, Z. U. Ahmad, Q. Y. Lian, L. G. Yao and M. E. Zappi, *Chem. Eng. J.*, 2021, **403**, 126286.
3 I. O. Saheed, W. D. Oh and F. B. M. Suah, *J. Hazard. Mater.*, 2021, **408**, 124889.
4 J. M. Herrmann, *Catal. Today*, 1999, **53**, 115–129.
5 T. O. Ajiboye, O. A. Oyewo and D. C. Onwudiwe, *Chemosphere*, 2021, **262**, 128379.
6 T. Lu, Q. Zhang, Z. Y. Zhang, B. L. Hu, J. M. Chen, J. Chen and H. F. Qian, *J. Environ. Sci.*, 2021, **99**, 175–186.
7 B. S. Rathi, P. S. Kumar and P. L. Show, *J. Hazard. Mater.*, 2021, **409**, 124413.
8 M. Nasrollahzadeh, M. Sajjadi, S. Iravani and R. S. Varma, *J. Hazard. Mater.*, 2021, **401**, 123401.
9 M. D. Regulacio and M. Y. Han, *Acc. Chem. Res.*, 2016, **49**, 511–519.
10 L. Cheng, L. Liu, K. Yan and J. D. Zhang, *Chem. Eng. J.*, 2017, **330**, 1380–1389.
11 R. C. Pawar, V. Khare and C. S. Lee, *Dalton Trans.*, 2014, **43**, 12514–12527.
12 G. S. Li, L. Wu, F. Li, P. P. Xu, D. Q. Zhang and H. X. Li, *Nanoscale*, 2013, **5**, 2118–2125.
13 Q. Li, X. Li, S. Wageh, A. A. Al-Ghamdi and J. G. Yu, *Adv. Energy Mater.*, 2015, **5**, 1500010.
14 M. Pelaez, N. T. Nolan, S. C. Pillai, M. K. Seery, P. Falaras, A. G. Kontos, P. S. M. Dunlop, J. W. J. Hamilton, J. A. Byrne, K. O'Shea, M. H. Entezari and D. D. Dionysiou, *Appl. Catal., B*, 2012, **125**, 331–349.
15 R. Asahi, T. Morikawa, T. Ohwaki, K. Aoki and Y. Taga, *Science*, 2001, **293**, 269–271.
16 R. Fiorenza, A. Di Mauro, M. Cantarella, C. Iaria, E. M. Scalisi, M. V. Brundo, A. Gulino, L. Spitaleri, G. Nicotra, S. Dattilo, S. C. Carroccio, V. Privitera and G. Impellizzeri, *Chem. Eng. J.*, 2020, **379**, 122309.
17 K. M. Lee, C. W. Lai, K. S. Ngai and J. C. Juan, *Water Res.*, 2016, **88**, 428–448.
18 A. Y. Zhang, W. K. Wang, D. N. Pei and H. Q. Yu, *Water Res.*, 2016, **92**, 78–86.
19 S. Raha and M. Ahmaruzzaman, *Chem. Eng. J.*, 2020, **387**, 123766.
20 A. Talaiekhozani, S. Rezania, K. H. Kim, R. Sanaye and A. M. Amani, *J. Cleaner Prod.*, 2021, **278**, 123895.
21 A. Serra, L. Philippe, F. Perreault and S. Garcia-Segura, *Water Res.*, 2021, **188**, 116543.
22 M. R. Hoffmann, S. T. Martin, W. Y. Choi and D. W. Bahnemann, *Chem. Rev.*, 1995, **95**, 69–96.
23 H. J. Zhang, G. H. Chen and D. W. Bahnemann, *J. Mater. Chem.*, 2009, **19**, 5089–5121.
24 R. Daghrir, P. Drogui and D. Robert, *J. Photochem. Photobiol., A*, 2012, **238**, 41–52.
25 C. C. Wang, J. R. Li, X. L. Lv, Y. Q. Zhang and G. S. Guo, *Energy Environ. Sci.*, 2014, **7**, 2831–2867.
26 J. M. Clemente-Juan, E. Coronado and A. Gaita-Arino, *Chem. Soc. Rev.*, 2012, **41**, 7464–7478.
27 J. Tucher, Y. Wu, L. C. Nye, I. Ivanovic-Burmazovic, M. M. Khusniyarov and C. Streb, *Dalton Trans.*, 2012, **41**, 9938–9943.
28 Q. Li and Y. Wei, *Chem. Commun.*, 2018, **54**, 1375–1378.
29 J. Chen, Y. Ma, D. Zhang, Y. Yang, M. K. Bera, J. Luo, E. Raee and T. Liu, *J. Coord. Chem.*, 2020, **73**, 2579–2589.
30 N. P. Martin and M. Nyman, *Angew. Chem., Int. Ed.*, 2021, **60**, 954–960.
31 F. Xin and M. T. Pope, *Organometallics*, 1994, **13**, 4881–4886.
32 P. Gouzerh and A. Proust, *Chem. Rev.*, 1998, **98**, 77–111.
33 S. A. Adonin, N. V. Izarova, C. Besson, P. A. Abramov, B. Santiago-Schubel, P. Kogerler, V. P. Fedin and M. N. Sokolov, *Chem. Commun.*, 2015, **51**, 1222–1225.
34 Z. Liang, T. Li, L. Zhang, L. Zheng, W. Jia and Q. Mao, *Inorg. Chem. Commun.*, 2020, **116**, 107895.
35 A. V. Anyushin, A. Kondinski and T. N. Parac-Vogt, *Chem. Soc. Rev.*, 2020, **49**, 382–432.
36 H. Li, H. Sun, W. Qi, M. Xu and L. Wu, *Angew. Chem., Int. Ed. Engl.*, 2007, **46**, 1300–1303.
37 W. Qi, Y. Wang, W. Li and L. Wu, *Chemistry*, 2010, **16**, 1068–1078.
38 J. W. Zhao, J. L. Zhang, Y. Z. Li, J. Cao and L. J. Chen, *Cryst. Growth Des.*, 2014, **14**, 1467–1475.
39 X. Wang, J. Sun, H. Lin, Z. Chang, G. Liu and X. Wang, *CrystEngComm*, 2017, **19**, 3167–3177.
40 A. Blazevic and A. Rompel, *Coord. Chem. Rev.*, 2016, **307**, 42–64.
41 W. W. Ayass, T. Fodor, E. Farkas, Z. Lin, H. M. Qasim, S. Bhattacharya, A. S. Mougharbel, K. Abdallah, M. S. Ullrich, S. Zaib, J. Iqbal, S. Harangi, G. Szalontai, I. Banyai, L. Zekany, I. Toth and U. Kortz, *Inorg. Chem.*, 2018, **57**, 7168–7179.
42 P. Wu, Y. Wang, W. Chen, X. Hu, B. Huang and Z. Xiao, *Inorg. Chem.*, 2021, **60**, 4347–4351.
43 Q. Li, L. Zhang, J. Dai, H. Tang, Q. Li, H. Xue and H. Pang, *Chem. Eng. J.*, 2018, **351**, 441–461.
44 D. Zang, Y. Huang, Q. Li, Y. Tang and Y. Wei, *Appl. Catal., B*, 2019, **249**, 163–171.
45 M. Wang, G. Q. Tan, M. Y. Dang, Y. Wang, B. X. Zhang, H. J. Ren, L. Lv and A. Xia, *J. Colloid Interface Sci.*, 2021, **582**, 212–226.
46 S. Fujimoto, J. M. Cameron, R. J. Wei, K. Kastner, D. Robinson, V. Sans, G. N. Newton and H. Oshio, *Inorg. Chem.*, 2017, **56**, 12169–12177.
47 Y. W. Liu, F. Luo, S. M. Liu, S. X. Liu, X. Y. Lai, X. H. Li, Y. Lu, Y. G. Li, C. W. Hu, Z. Shi and Z. P. Zheng, *Small*, 2017, **13**, 1603174.
48 J. J. Jiang, X. Y. Wang, Y. Liu, Y. H. Ma, T. R. Li, Y. H. Lin, T. F. Xie and S. S. Dong, *Appl. Catal., B*, 2020, **278**, 119349.
49 J. L. Wang and L. J. Xu, *Crit. Rev. Environ. Sci. Technol.*, 2012, **42**, 251–325.
50 G. Marci, E. I. Garcia-Lopez and L. Palmisano, *Eur. J. Inorg. Chem.*, 2014, **2014**, 21–35.
51 H. An, Y. Hu, L. Wang, E. Zhou, F. Fei and Z. Su, *Cryst. Growth Des.*, 2015, **15**, 164–175.
52 Y. Hua, G. Chen, X. Xu, X. Zou, J. Liu, B. Wang, Z. Zhao, Y. Chen, C. Wang and X. Liu, *J. Phys. Chem. C*, 2014, **118**, 8877–8884.
53 Y. Hua, C. Wang, J. Liu, B. Wang, X. Liu, C. Wu and X. Liu, *J. Mol. Catal. A: Chem.*, 2012, **365**, 8–14.

54 Z. Garazhian, A. Rezaeifard, M. Jafarpour and A. Farrokhi, *ACS Appl. Nano Mater.*, 2020, **3**, 648–657.
55 X. S. Yu, H. J. Cui, Q. Z. Wang, J. S. Li, F. Su, L. C. Zhang, X. J. Sang and Z. M. Zhu, *Appl. Organomet. Chem.*, 2020, **34**, e5720.
56 L. Cademartiri and V. Kitaev, *Nanoscale*, 2011, **3**, 3435–3446.
57 X. Li, H. Xue and H. Pang, *Nanoscale*, 2017, **9**, 216–222.
58 T. Wei, M. Zhang, P. Wu, Y. J. Tang, S. L. Li, F. C. Shen, X. L. Wang, X. P. Zhou and Y. Q. Lan, *Nano Energy*, 2017, **34**, 205–214.
59 H. Guo, C. Gong, X. Zeng, H. Xu, Q. Zeng, J. Zhang, Z. Zhong and J. Xie, *Dalton Trans.*, 2019, **48**, 5541–5550.
60 S. U. Khan, M. Akhtar, F. U. Khan, J. Peng, A. Hussain, H. F. Shi, J. Du, G. Yan and Y. G. Li, *J. Coord. Chem.*, 2018, **71**, 2604–2621.
61 H. Zhang, J. Yang, Y. Y. Liu, S. Y. Song, X. L. Liu and J. F. Ma, *Dyes Pigm.*, 2016, **133**, 189–200.
62 K. Nakata and A. Fujishima, *J. Photochem. Photobiol., C*, 2012, **13**, 169–189.
63 S. W. Verbruggen, *J. Photochem. Photobiol., C*, 2015, **24**, 64–82.
64 Q. Guo, C. Y. Zhou, Z. B. Ma and X. M. Yang, *Adv. Mater.*, 2019, **31**, 26.
65 R. Sivakumar, J. Thomas and M. Yoon, *J. Photochem. Photobiol., C*, 2012, **13**, 277–298.
66 L. Li, Y. L. Yang, R. Q. Fan, J. Liu, Y. X. Jiang, B. Yang and W. W. Cao, *Dalton Trans.*, 2016, **45**, 14940–14947.
67 E. Rafiee, N. Pami, A. A. Zinatizadeh and S. Eavani, *J. Photochem. Photobiol., A*, 2020, **386**, 112145.
68 C. E. Diaz-Uribe, A. Rodriguez, D. Utria, W. Vallejo, E. Puello, X. Zarate and E. Schott, *Polyhedron*, 2018, **149**, 163–170.
69 S. Q. Zhang, L. Chen, H. B. Liu, W. Guo, Y. X. Yang, Y. H. Guo and M. X. Huo, *Chem. Eng. J.*, 2012, **200**, 300–309.
70 X. Q. An, Q. W. Tang, H. C. Lan, H. J. Liu and J. H. Qu, *Appl. Catal., B*, 2019, **244**, 407–413.
71 Z. Yang, S. Gao, H. Li and R. Cao, *J. Colloid Interface Sci.*, 2012, **375**, 172–179.
72 E. Rafiee, E. Noori, A. A. Zinatizadeh and H. Zanganeh, *J. Mater. Sci.: Mater. Electron.*, 2018, **29**, 20668–20679.
73 S. Zhang, L. Chen, H. Liu, W. Guo, Y. Yang, Y. Guo and M. Huo, *Chem. Eng. J.*, 2012, **200–202**, 300–309.
74 K. Li, Y. Guo, F. Ma, H. Li, L. Chen and Y. Guo, *Catal. Commun.*, 2010, **11**, 839–843.
75 R. Khoshnavazi, H. Sohrabi, L. Bahrami and M. Amiri, *J. Sol-Gel Sci. Technol.*, 2017, **8**, 332–341.
76 P. Wu, Q. Xue, J. Liu, T. Wang, C. Feng, B. Liu, H. Hu and G. Xue, *ChemCatChem*, 2021, **13**, 388–396.
77 A. Pearson, H. Zheng, K. Kalantar-zadeh, S. K. Bhargava and V. Bansal, *Langmuir*, 2012, **28**, 14470–14475.
78 Y. C. Lopez, H. Viltres, N. K. Gupta, P. Acevedo-Pena, C. Leyva, Y. Ghaffari, A. Gupta, S. Kim, J. Bae and K. S. Kim, *Environ. Chem. Lett.*, 2021, **19**, 1295–1334.
79 G. Paille, M. Gomez-Mingot, C. Roch-Marchal, B. Lassalle-Kaiser, P. Mialane, M. Fontecave, C. Mellot-Draznieks and A. Dolbecq, *J. Am. Chem. Soc.*, 2018, **140**, 3613–3618.
80 X. X. Li, J. Liu, L. Zhan, L. Z. Dong, Z. F. Xin, S. L. Li, X. Q. Huang Fu, K. Huang and Y. Q. Lan, *ACS Appl. Mater. Interfaces*, 2019, **11**, 25790–25795.
81 X. J. Kong, Z. Lin, Z. M. Zhang, T. Zhang and W. Lin, *Angew. Chem., Int. Ed.*, 2016, **55**, 6411–6416.
82 B. Cong, Z. Su, Z. Zhao, W. Zhao and X. Ma, *J. Coord. Chem.*, 2018, **71**, 411–420.
83 H. F. Hao, W. Z. Zhou, H. Y. Zang, H. Q. Tan, Y. F. Qi, Y. H. Wang and Y. G. Li, *Chem.–Asian J.*, 2015, **10**, 1676–1683.
84 B. Liu, Z. T. Yu, J. Yang, W. Hua, Y. Y. Liu and J. F. Ma, *Inorg. Chem.*, 2011, **50**, 8967–8972.
85 X. Wang, Z. Chang, H. Lin, A. Tian, G. Liu and J. Zhang, *Dalton Trans.*, 2014, **43**, 12272–12278.
86 J. Wang, D. Zhou, G. L. Wang, L. Lu, Y. Pan, A. Singh and A. Kumar, *Inorg. Chim. Acta*, 2019, **492**, 186–191.
87 J. Q. Sha, X. Y. Yang, N. Sheng, G. D. Liu, J. S. Li and J. B. Yang, *J. Solid State Chem.*, 2018, **263**, 52–59.
88 J. Guo, J. Yang, Y. Y. Liu and J. F. Ma, *CrystEngComm*, 2012, **14**, 6609–6617.
89 X. L. Wang, C. H. Gong, J. W. Zhang, G. C. Liu, X. M. Kan and N. Xu, *CrystEngComm*, 2015, **17**, 4179–4189.
90 X. Wang, J. Sun, H. Lin, Z. Chang, G. Liu and X. Wang, *RSC Adv.*, 2016, **6**, 110583–110591.
91 Y. H. Luo, Z. L. Lang, X. X. Lu, W. W. Ma, Y. Xu and H. Zhang, *Inorg. Chem. Commun.*, 2016, **72**, 13–16.
92 X. L. Hao, Y. Y. Ma, Y. H. Wang, W. Z. Zhou and Y. G. Li, *Inorg. Chem. Commun.*, 2014, **41**, 19–24.
93 X. Sun, J. Zhang and Z. Fu, *ACS Appl. Mater. Interfaces*, 2018, **10**, 35671–35675.
94 N. Du, L. Gong, L. Fan, K. Yu, H. Luo, S. Pang, J. Gao, Z. Zheng, J. Lv and B. Zhou, *ACS Appl. Nano Mater.*, 2019, **2**, 3039–3049.
95 X. Wang, Z. Chang, H. Lin, A. Tian, G. Liu, J. Zhang and D. Liu, *RSC Adv.*, 2015, **5**, 14020–14026.
96 S. R. Koohi, S. Allahyari, D. Kahforooshan, N. Rahemi and M. Tasbihi, *J. Inorg. Organomet. Polym. Mater.*, 2019, **29**, 365–377.
97 Y. Wang, X. Wang and M. Antonietti, *Angew. Chem., Int. Ed.*, 2012, **51**, 68–89.
98 J. Zhang, Y. Chen and X. Wang, *Energy Environ. Sci.*, 2015, **8**, 3092–3108.
99 M. Groenewolt and M. Antonietti, *Adv. Mater.*, 2005, **17**, 1789–1792.
100 K. Li, L. Yan, Z. Zeng, S. Luo, X. Luo, X. Liu, H. Guo and Y. Guo, *Appl. Catal., B*, 2014, **156**, 141–152.
101 S. Zhao, X. Zhao, H. Zhang, J. Li and Y. Zhu, *Nano Energy*, 2017, **35**, 405–414.
102 J. Liu, S. Xie, Z. Geng, K. Huang, L. Fan, W. Zhou, L. Qiu, D. Gao, L. Ji, L. Duan, L. Lu, W. Li, S. Bai, Z. Liu, W. Chen, S. Feng and Y. Zhang, *Nano Lett.*, 2016, **16**, 6568–6575.
103 J. He, H. Sun, S. Indrawirawan, X. Duan, M. O. Tade and S. Wang, *J. Colloid Interface Sci.*, 2015, **456**, 15–21.
104 K. S. Novoselov, Z. Jiang, Y. Zhang, S. V. Morozov, H. L. Stormer, U. Zeitler, J. C. Maan, G. S. Boebinger, P. Kim and A. K. Geim, *Science*, 2007, **315**, 1379.

105 H. Li, S. Pang, S. Wu, X. Feng, K. Muellen and C. Bubeck, *J. Am. Chem. Soc.*, 2011, **133**, 9423–9429.
106 Y. Ji, L. Huang, J. Hu, C. Streb and Y. F. Song, *Energy Environ. Sci.*, 2015, **8**, 776–789.
107 R. Wang, L. Dang, Y. Liu and W. Jiao, *Adv. Powder Technol.*, 2019, **30**, 1400–1408.
108 G. Aragay, F. Pino and A. Merkoci, *Chem. Rev.*, 2012, **112**, 5317–5338.
109 M. Hadei, A. Mesdaghinia, R. Nabizadeh, A. H. Mahvi, S. Rabbani and K. Naddafi, *Environ. Sci. Pollut. Res.*, 2021, **28**, 13055–13071.
110 T. Ahamad, M. Naushad, S. I. Al-Saeedi, S. Almotairi and S. M. Alshehri, *Mater. Lett.*, 2020, **263**, 127271.
111 M. Ghali, C. Brahmi, M. Benltifa, F. Dumur, S. Duval, C. Simonnet Jegat, F. Morlet-Savary, S. Jellali, L. Bousselmi and J. Lalevee, *J. Polym. Sci., Part A: Polym. Chem.*, 2019, **57**, 1538–1549.
112 S. Antonaraki, T. M. Triantis, E. Papaconstantinou and A. Hiskia, *Catal. Today*, 2010, **151**, 119–124.
113 C. Feng, Y. Li and X. Liu, *Chin. J. Chem.*, 2012, **30**, 127–132.
114 E. S. Da Silva, M. Sarakha, H. D. Burrows and P. Wong Wah Chung, *J. Photochem. Photobiol., A*, 2017, **334**, 61–73.
115 P. Meng, J. Huang and X. Liu, *Appl. Surf. Sci.*, 2019, **465**, 125–135.
116 P. Meng, J. Huang and X. Liu, *J. Colloid Interface Sci.*, 2019, **551**, 208–218.
117 R. Kaveh and H. Alijani, *J. Asian Ceram. Soc.*, 2021, **9**, 343–365.
118 H. Shi, T. Zhao, J. Wang, Y. Wang and Y. Li, *J. Alloys Compd.*, 2020, **860**, 157924.
119 M. Bonchio, M. Carraro, G. Scorrano and A. Bagno, *Adv. Synth. Catal.*, 2004, **346**, 648–654.
120 L. Hao, M. Hu, X. Xiong and Y. Xu, *Photochem. Photobiol. Sci.*, 2016, **15**, 1299–1303.
121 M. Hu and Y. Xu, *Chem. Eng. J.*, 2014, **246**, 299–305.
122 L. Yao, L. Z. Zhang, R. Wang, C. H. Loh and Z. L. Dong, *Sep. Purif. Technol.*, 2013, **118**, 162–169.
123 J. Yu, T. Wang and S. Rtimi, *Appl. Catal., B*, 2019, **254**, 66–75.
124 S. Babić, L. Ćurković, D. Ljubas and M. Čizmić, *Curr. Opin. Green Sustain. Chem.*, 2017, **6**, 34–41.
125 R. He, K. Xue, J. Wang, Y. Yan, Y. Peng, T. Yang, Y. Hu and W. Wang, *Chemosphere*, 2020, **259**, 127465.
126 J. J. Walsh, A. M. Bond, R. J. Forster and T. E. Keyes, *Coord. Chem. Rev.*, 2016, **306**, 217–234.
127 B. Huang, D. H. Yang and B. H. Han, *J. Mater. Chem. A*, 2020, **8**, 4593–4628.
128 B. Huang, Y. Ma, Z. Xiong, Z. Xiao, P. Wu, P. Jiang and M. Liang, *Energy Environ. Mater.*, 2020, DOI: 10.1002/eem2.12150.
129 H. Li, Y. Zhao, C. Yin, L. Jiao and L. Ding, *Colloids Surf., A*, 2019, **572**, 147–151.
130 J. X. Liu, X. B. Zhang, Y. L. Li, S. L. Huang and G. Y. Yang, *Coord. Chem. Rev.*, 2020, **414**, 213260.
131 D. Y. Du, J. S. Qin, S. L. Li, Z. M. Su and Y. Q. Lan, *Chem. Soc. Rev.*, 2014, **43**, 4615–4632.